ELSEVIER

Thermochimica Acta 401 (2003) 121–130

thermochimica acta

www.elsevier.com/locate/tca

Dehydration of synthetic and natural vivianite

Ray L. Frost*, Matt L. Weier, Wayde Martens, J. Theo Kloprogge, Zhe Ding

Centre for Instrumental and Developmental Chemistry, Queensland University of Technology, GPO Box 2434, Brisbane, Qld 4001, Australia

Received 9 July 2002; received in revised form 11 October 2002; accepted 14 October 2002

Abstract

Thermal analyses of synthetic and natural vivianite (Fe^{2+})$_3$(PO$_4$)$_2$·8H$_2$O) were determined using a high-resolution thermal analyser coupled to a mass spectrometer.

Five dehydration weight loss steps were observed for the natural vivianite at 105, 138, 203, 272 and 437 °C. The first weight loss step involves the reaction (Fe^{2+})$_3$(PO$_4$)$_2$ · 8H$_2$O → (Fe^{2+})$_3$(PO$_4$)$_2$ · 3H$_2$O + 5H$_2$O. The TGA/MS for the synthetic vivianite gave similar results to that of the natural sample. Mass spectrometry shows that water is lost up to 450 °C and after this temperature oxygen is lost. Changes in the structure of vivianite were followed using infrared emission spectroscopy. A model is proposed for the dehydration of vivianite.

Keywords: Vivianite; Iron; Phosphate; Thermal analysis; Infrared emission spectroscopy

1. Introduction

The minerals may be divided into two groups according to the oxyanion being either arsenate or phosphate [1]. The phosphates in this mineral group are aruptite (Ni_3^{2+}(PO$_4$)$_2$·8H$_2$O), vivianite (Fe_3^{2+}(PO$_4$)$_2$·8H$_2$O), baricite ((Mg, Fe^{2+})$_3$(PO$_4$)$_2$·8H$_2$O) and bobierrite (Mg_3^{2+}(PO$_4$)$_2$·8H$_2$O). The mineral vivianite is of interest because of the possibility of formation in environmental situations such as in the coatings of water pipes and in soils from peat bogs, morasses and sediments. A blue encrustation was found on the repatriated remains of three US servicemen listed as missing in action (MIA) from Vietnam after 28 years. The identification and origin of the blue material was determined. Scanning electron microscopy with energy dispersive analysis and powder X-ray diffraction identified the material as the mineral vivianite, Fe$_3$(PO$_4$)$_2$·8H$_2$O [2]. It is possible that the minerals can be formed from aqueous solutions from ground waters and precipitated from solutions in sediments and soils. Evidence for the formation in soils is also known. If ground water is high in both Mg and Fe^{2+} then it is possible that both the minerals of the vivianite group such as baricite and bobierrite may form, particularly when phosphate fertilisers have been used in the surrounding farmlands. In fact, these minerals have been found in sediments in New Zealand. Our interest in the mineral vivianite arose because of the observation of some blue materials found in some acid drainage soils in both the Shoalhaven Plateau in NSW, Australia and in some soils drainage materials in South Australia.

Some infrared data exists for the vivianite phosphate minerals. Whilst the infrared spectra of some minerals have been forthcoming, few comprehensive studies of the vivianite related minerals such as divalent cationic phosphates have been undertaken [2]. Most of the

* Corresponding author. Tel.: +61-7-3864-2407; fax: +61-7-3864-1804.
E-mail address: r.frost@qut.edu.au (R.L. Frost).

0040-6031/03/$ – see front matter
PII: S0040-6031(02)00505-1

infrared data predates the advent of Fourier transform infrared spectroscopy [3–8]. Although some Raman studies of the vivianite phosphate minerals have been undertaken [9,10], no Raman spectroscopic investigation of these phosphate phase related minerals has been forthcoming. The Raman spectra of the tetrahedral anions in aqueous systems are well known. The symmetric stretching vibration of the phosphate anion (ν_1) is observed at 938 cm^{-1}, the asymmetric stretching mode (ν_3) at 1018 cm^{-1}. The ν_2 mode is observed at 420 cm^{-1} and the ν_4 mode at 567 cm^{-1}. Farmer lists a number of infrared spectra of phosphates including vivianite [2]. The symmetric stretching mode was not listed but the antisymmetric mode was found at 990 and 1040 cm^{-1}. Bands at 890 and 872 cm^{-1} were not assigned. Bands for the ν_4 mode was observed at 475, 560 and 590 cm^{-1}.

Some thermal analysis studies of the vivianite mineral have been undertaken [11–15]. Pulou suggested that like the arsenates, the phosphates have a strong endothermic peak at 250 °C due to dehydration and oxidation, followed by an exothermic peak attributed to recrsytallisation. Differential thermal analysis can distinguish between the phosphates of Ni, Co, and (Mg or Fe), the exothermic peaks occurring at 600 °C (Co), 760 °C (Ni), 675 °C (Co/Ni = 1), 720 °C (Co/Ni = 1/3), 650 °C (bobierrite), 620 °C (Co/Mg = 1), and 650 °C (vivianite) [13]. Vivianite was found to show a major differential thermal response over the 65–316 °C attributable to an endothermic loss of structural water, combined with the oxidation of Fe^{2+} (which results in exothermic peak(s)), and consequent breakdown of the original structure. Subsequently, a gradual sintering of the amorphous product culminates in an exothermic structural ordering at 660 °C., resulting in the formation of α-$FePO_4$, $Fe(PO_3)_3$, and, occasionally, Fe_2O_3 [15]. In this work we undertake a thermal study of the mineral vivianite using a combination of high-resolution TGA coupled to a mass spectrometer and infrared emission spectroscopy.

2. Experimental

2.1. Natural and synthetic vivianite

The natural vivianite mineral was obtained from BK minerals suppliers and was composed of large deep-blue prismatic crystals. The mineral originated from the Ukraine. Synthetic vivianite iron(II) phosphate Fe was prepared by the slow addition of the 3.5×10^{-3} M ferrous sulphate solution to a very dilute 5.0×10^{-3} M sodium phosphate solution using a peristaltic pump at 70 °C. The hydrated synthetic vivianite precipitated from the solution and were filtered and dried. Samples were analysed for phase purity by X-ray diffraction and for chemical composition by ICP-AES and also by electron probe analyses. Both the natural and synthetic minerals were found to be phase pure.

2.2. Thermal analysis

Thermal decomposition of the hydrotalcite was carried out in a TA® Instruments incorporated high-resolution thermogravimetric analyser (series Q500) in a flowing nitrogen atmosphere (80 cm^3/min). Approximately 5 mg of sample was heated in an open platinum crucible at a rate of 2.0 °C/min up to 500 °C. With the quasi-isothermal, quasi-isobaric heating program of the instrument the furnace temperature was regulated precisely to provide a uniform rate of decomposition in the main decomposition stage. The TGA instrument was coupled to a Balzers (Pfeiffer) mass spectrometer for gas analysis. Only selected gases were analysed.

2.3. Infrared emission spectroscopy

FTIR emission spectroscopy was carried out on a Nicolet spectrometer equipped with a TGS detector, which was modified by replacing the IR source with an emission cell. A description of the cell and principles of the emission experiment have been published elsewhere [16–23]. Approximately 0.2 mg of vivianite mineral was spread as a thin layer (approximately 0.2 μm) on a 6 mm diameter platinum surface and held in an inert atmosphere within a nitrogen-purged cell during heating.

In the normal course of events, three sets of spectra are obtained: firstly the black body radiation over the temperature range selected at the various temperatures, secondly the platinum plate radiation is obtained at the same temperatures and thirdly the spectra from the platinum plate covered with the sample. Normally only one set of black body and platinum radiation is

required. The emittance spectrum (E) at a particular temperature was calculated by subtraction of the single beam spectrum of the platinum backplate from that of the platinum (Pt) + sample (S), and the result ratioed to the single beam spectrum of an approximate blackbody (graphite (C)). The following equation was used to calculate the emission spectra.

$$E = -0.5^{*} \log \frac{\mathrm{Pt} - \mathrm{S}}{\mathrm{Pt} - \mathrm{C}}$$

This spectral manipulation is carried out after all the spectral data has been collected. The emission spectra were collected at intervals of 50 °C over the range 200–750 °C. The time between scans (while the temperature was raised to the next hold point) was approximately 100 s. It was considered that this was sufficient time for the heating block and the powdered sample to reach temperature equilibrium. The spectra were acquired by coaddition of 64 scans for the whole temperature range (approximate scanning time 45 s), with a nominal resolution of 4 cm^{-1}. Good quality spectra can be obtained providing the sample thickness is not too large. If too large a sample is used then the spectra become difficult to interpret because of the presence of combination and overtone bands. Spectral manipulation such as baseline adjustment, smoothing and normalisation was performed using the GRAMS® software package (Galactic Industries Corporation, Salem, NH, USA).

3. Results and discussion

3.1. Thermogravimetry

The thermogravimetric and differential thermogravimetry of synthetic and natural vivianite are shown in Fig. 1. Multiple weight loss steps are observed for both the synthetic and natural vivianites. The synthetic vivianite differs from the natural sample in that adsorbed water around 4 wt.% is lost at around 50 °C. The synthetic vivianite displays weight loss steps at 105, 134, 193 and 260 °C in the temperature range below 300 °C. The natural vivianite shows weight loss steps at 105, 138, 203 and 272 °C below 300 °C. These weight loss steps are attributed to dehydration. The percentage weight loss at 105 °C for the synthetic vivianite is 13.0% compared with a value of 19.4% for the natural vivianite. The theoretical weight loss due to dehydration based upon the formulae ($Fe_3^{2+}(PO_4)_2 \cdot 8H_2O$) is 28.72%, i.e. 3.339% per water molecule. The weight loss for the first step for vivianite is 13.0%. This value would suggest that 4 mol water are lost at 105 °C. However, the weight loss for the first step for the natural vivianite is 19.4%, which suggests 5 mol water are lost in this dehydration step.

Over the temperature range 110–300 °C (as mass spectrometry shows) water appears to be lost continuously for the synthetic vivianite and a weight loss of 9.6% is observed over this temperature range. This weight loss suggests that a total of 3 mol water are lost in several stages. The total weight loss for dehydration is 22.6% a value, which does not compare well with the theoretical value of 28.7%. However, if the weight loss of water below 100 °C is included in the dehydration weight loss then a value of 26.6% is obtained. The weight loss steps for the synthetic vivianite are not as well defined as for the natural sample. For the natural vivianite, the well defined weight loss steps at 138, 203, 272 and 437 °C have weight losses of 1.1, 3.43, 2.59and 1.64%. This makes a total weight loss of 8.76% for these steps, which together with the weight loss of 19.4% makes a total dehydration weight loss of 28.16%. This value compares well with the theoretical weight loss of 28.72%.

Weight loss steps at higher temperatures are observed. For the synthetic vivianite these are observed at 449, 524 °C and a series of steps centred on 850 °C. A single weight loss step at 437 °C is observed for the natural vivianite. MS suggests that this weight loss is attributable to water loss and not oxygen loss. The high temperature weight loss observed for the synthetic vivianite was not observed for the natural vivianite although it is suspected that the step may be starting to be observed at 1000 °C, the upper temperature limit of the TGA furnace. MS shows that this weight loss may be ascribed to oxygen. The high temperature weight loss steps are attributed to oxygen loss.

3.2. Mass spectrometric analysis

The mass spectra of oxygen and water loss are shown in Fig. 2. The mass gain of water in the MS spectrometer corresponds with precision the DTGA pattern for both the synthetic and natural vivianite.

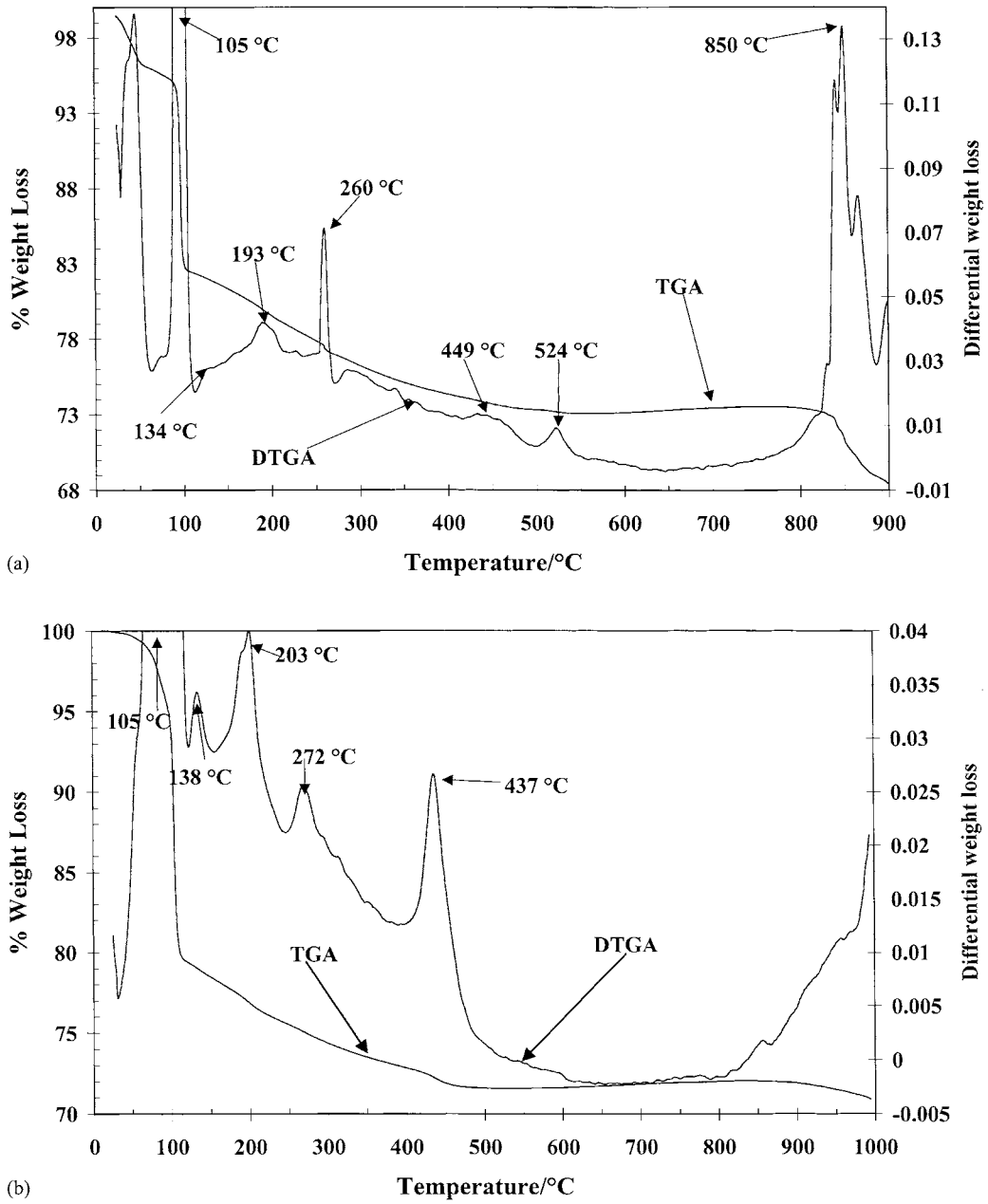

Fig. 1. TGA and DGTA of (a) synthetic vivianite; (b) natural vivianite.

The mass spectrum confirms the observation of the weight loss steps as being due to water loss. The mass spectrum of oxygen shows that the higher temperature weight loss steps are due to oxygen mass loss. Both the TGA/DTGA and DTGA/MS patterns for the natural and synthetic vivianite are different. Although the weight loss steps are identical. This difference is attributed to the lack of crystallinity in the synthetic vivianite. The synthesised vivianite mineral was hydrothermally treated for at 70 °C for 14 days to achieve

Ostwald ripening. However, this was not successful because prolonged thermal treatment resulted in the formation of the monohydrate.

There have been some studies on the dehydration of vivianite [24,25]. Kotlova et al. suggested that the dehydration of vivianite occurred in three X-ray amorphous stages at 230–260° where 5 mol H_2O were lost, 330–345° where 2 mol H_2O were lost and 380–420° where 1 mol H_2O was lost. The anhydride, a non-identifiable Fe(III)-phosphate modification was

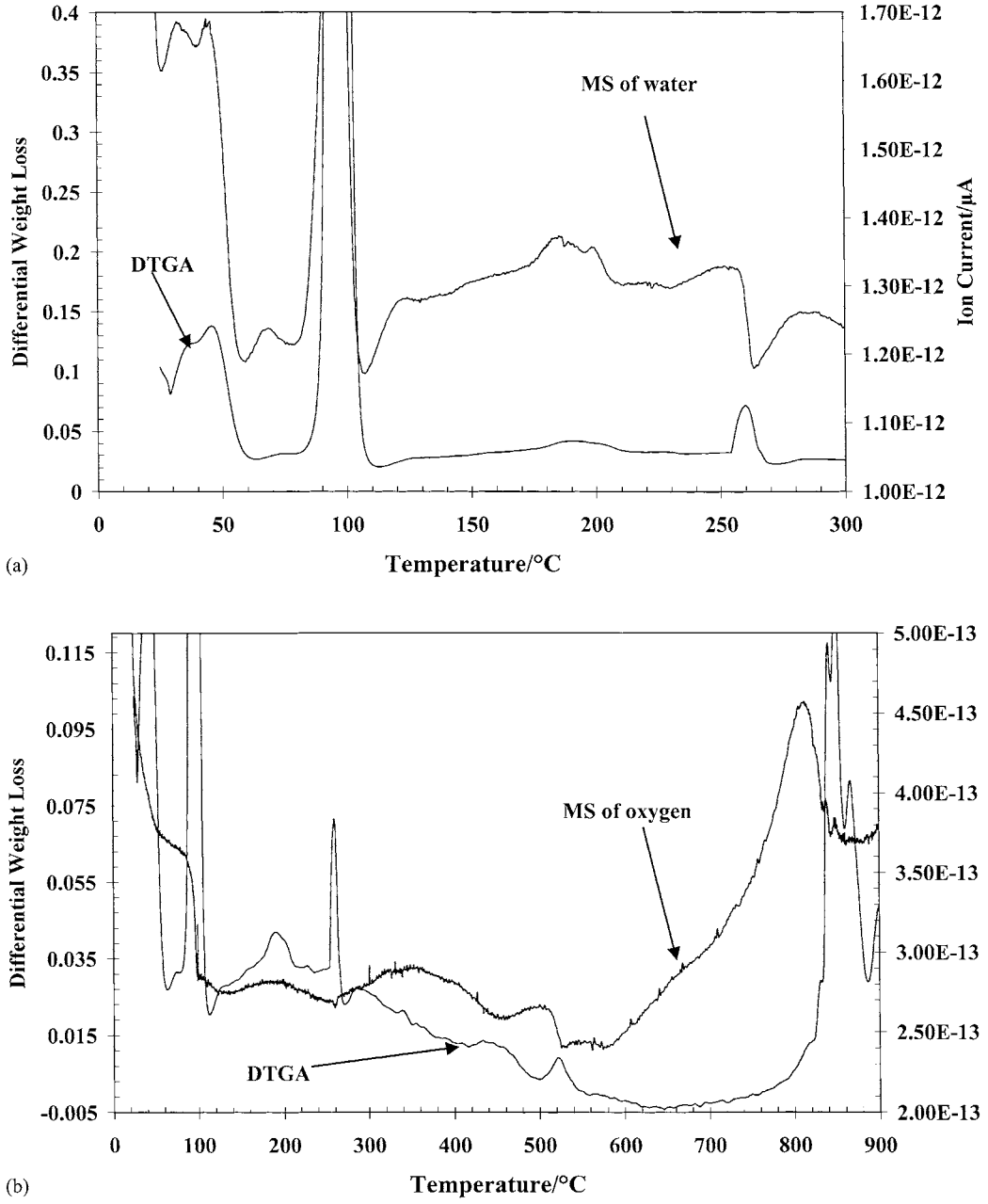

Fig. 2. DTGA and MS of (a) water; (b) oxygen for synthetic vivianite; (c) DTGA and MS of water for natural vivianite.

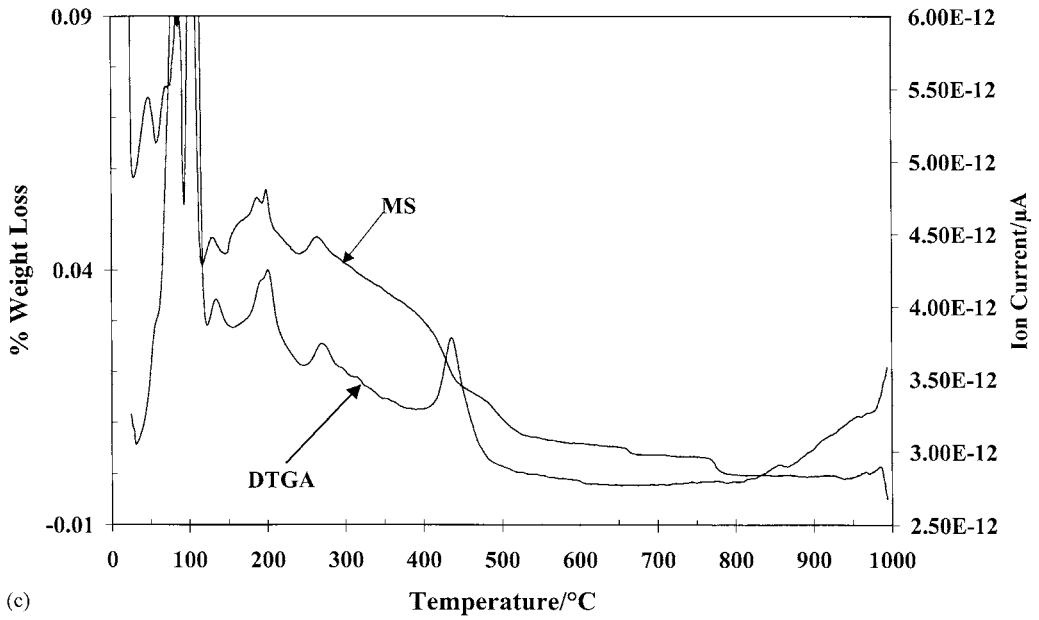

Fig. 2. (*Continued*).

not recognised by X-ray analysis; the transformation began at 260° and was completed at 550–560° to give the Fe(III)-phosphate modification. The latter remained stable after cooling to room temperature [24]. These results differ from the values in this research. The differences in results may be attributed to the techniques used for the thermal analysis. Kotlova et al. used DTA in combination with X-ray diffraction. In this work we are using high-resolution thermogravimetry in conjunction with mass spectrometry. What is interesting is that Kotlova et al. found a high temperature dehydration step at 380–420 °C. This value corresponds well with the final dehydration step observed in this work. Figueiredo et al. [25] showed the thermal breakdown (400–500°) of vivianite by dehydration and total Fe oxidation gives rise to an amorphous material, in which Fe(III) is distributed between octahedral and tetrahedral sites. A complex mixture of phases was found above 600–650 °C. Berlinite-type $FePO_4$ was formed. Further heating resulted in the formation of Fe_3PO_7 [25].

3.3. Model for the dehydration of vivianite

The following series of reactions is a model based upon the weight loss of water for the natural vivianite. The synthetic vivianite results were not sued for this model as the data differed form that of the natural sample. The DTGA curve was band fitted and the area under the bands was used to calculate percentage weight loss. This was then normalised and converted to the nearest mole of water. The values obtained for the five weight loss steps were 4.6, 0.45, 0.84, 0.98 and 0.45 which gave moles of water as 5, 0.5, 1, 1 and 0.5, respectively. Thus, these values are used in the following model for the dehydration of vivianite.

Step 1 (105 °C):

$$(Fe^{2+})_3(PO_4)_2 \cdot 8H_2O \rightarrow (Fe^{2+})_3(PO_4)_2 \cdot 3H_2O + 5H_2O$$

Step 2 (138 °C):

$$(Fe^{2+})_3(PO_4)_2 \cdot 3H_2O \rightarrow (Fe^{2+})_3(PO_4)_2 \cdot 2.5H_2O + 0.5H_2O$$

Step 3 (203 °C):

$$(Fe^{2+})_3(PO_4)_2 \cdot 2.5H_2O \rightarrow (Fe^{2+})_3(PO_4)_2 \cdot 1.5H_2O + 1H_2O$$

Table 1
Results of the infrared emission spectra of the hydroxyl stretching region of vivianite

Temperature (°C)	Peak position					
100	3488 (10.9)	3449 (38.8)	3238 (19.5)		2924 (1.1)	2858 (0.45)
150	3493 (19.4)	3425 (0.24)	3375 (31.3)	3123 (4.26)	2912 (1.19)	2854 (0.410
200	3492 (13.4)	3437 (0.86)	3349 (20.9)	3160 (4.1)	2924 (1.9)	2860 (0.64)
250	3509 (8.3)	3438 (3.0)	3382 (17.3)	3197 (5.6)	2923 (1.6)	2861 (0.51)
300	3516 (9.2)	3414 (5.5)	3376 (11.5)	3171 (2.4)	2917 (1.5)	2861 (0.39)
350	3518 (5.1)	3422 7.0)	3258 (3.3)		2927 (1.2)	
400	3510 (1.2)	3401 (1.9)		3014 (1.37)	2961 (0.03)	

Values in parentheses are percentage relative area.

Step 4 (272 °C):

$$(Fe^{2+})_3(PO_4)_2 \cdot 1.5H_2O \rightarrow (Fe^{2+})_3(PO_4)_2 \cdot 0.5H_2O + 1H_2O$$

Step 5 (437 °C):

$$(Fe^{2+})_3(PO_4)_2 \cdot 0.5H_2O \rightarrow (Fe^{2+})_3(PO_4)_2 + 0.5H_2O$$

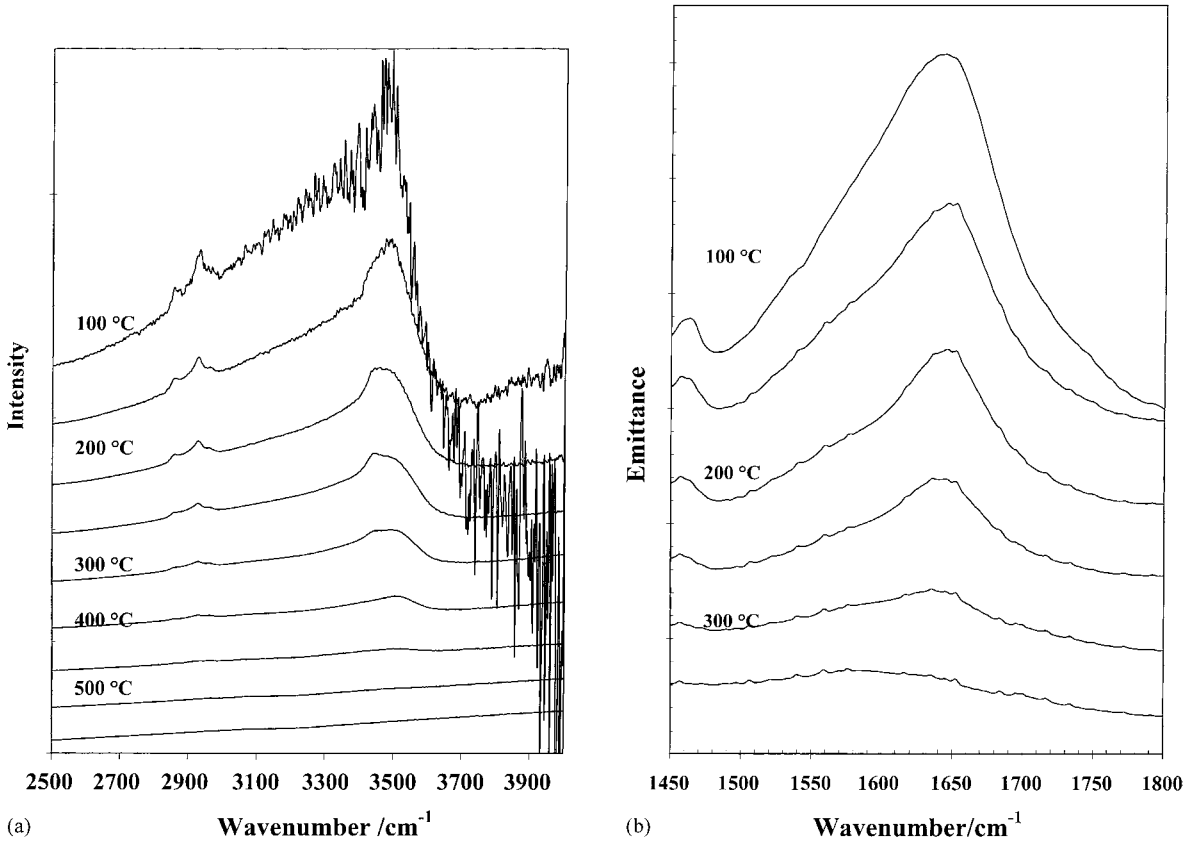

Fig. 3. Infrared emission spectra of (a) hydroxyl stretching region; (b) water bending region; (c) phosphate stretching region of synthetic vivianite.

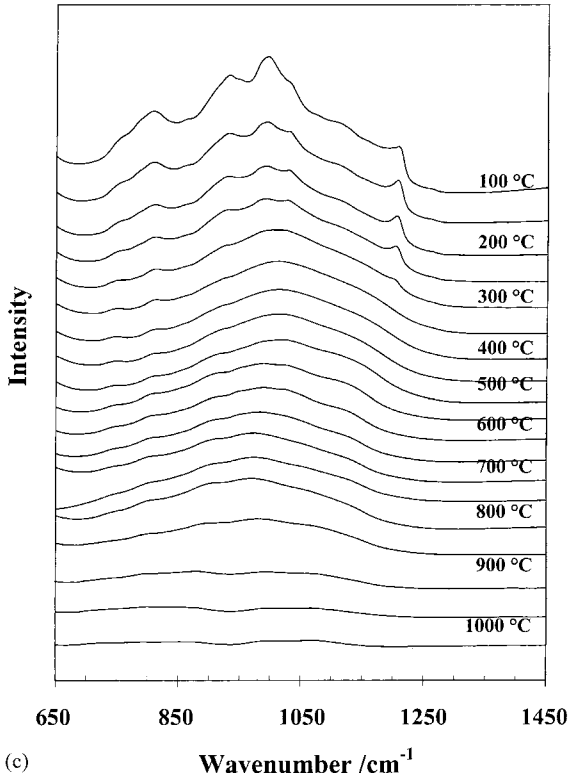

Fig. 3. (*Continued*).

The dehydration of vivianite is complex and occurs over five steps. This model differs from previously published work. The HR DTGA enabled more definitive interpretation of the weight loss steps.

3.4. Infrared emission spectroscopy

The infrared emission spectra of vivianite were used to confirm the weight loss of water and the spectra are shown in Fig. 3. The results of the band component analysis of the spectral regions as a function of temperature are shown in Table 1. Bands are curve resolved at 3488, 3449, 3238 cm^{-1} and also 2924 and 2858 cm^{-1}. The latter two bands are attributed to organic impurities. The intensity of these bands approach zero by 400 °C. The first three bands are assigned to water OH stretching vibrations. Vivianite shows three well-resolved bands in the Raman spectrum of the hydroxyl-stretching region at 3496, 3262 and 3130 cm^{-1}. In the infrared absorption spectrum of vivianite, hydroxyl stretching bands are observed at 3460, 3281 and 3104 cm^{-1}. A previous study gave bands at 3475, 3260 and 3125 cm^{-1}, which are in reasonable agreement with this work, considering the breadth of the bands in the hydroxyl-stretching region [9,26]. The intensity of the infrared emission bands decrease in intensity with increasing temperature until at 400 °C no intensity remains in the bands (Table 2). The loss of intensity of the OH stretching bands

Table 2
Results of the infrared emission spectra of the HOH bending modes of vivianite

Temperature (°C)	Peak position	
100	1646 (0.52)	1617 (3.7)
150	1650 (0.56)	1620 (3.13)
200	1643 (2.9)	
250	1641 (2.23)	
300	1624 (1.9)	
350	1608 (1.7)	
400	Not observed	

Values in parentheses are percentage relative area.

Table 3
Results of the infrared emission spectra of the phosphate bands of vivianite

Temperature (°C)	Peak position												
100	1459.(0.15)	1422 (0.25)	1209 (0.34)			1120 (0.83)	1083 (5.2)	1015 (1.5)	994 (3.3)	923 (7.5)	846 (0.56)	802 (2.4)	750
150	1461.(0.07)	1417 (0.11)	1209 (0.52)		1166 (6.4)	1115 (0.93)	1062 (7.6)	1029 (2.1)	992 (4.0)	923 (4.0)	873 (1.2)	804 (3.0)	750 (0.5)
200	1458.(0.08)	1427 (0.087)	1207 (0.62)	1200 (0.93)	1167 (9.65)	1116 (2.3)	1054 (13.0)	1014 (1.86)	990 (5.5)	922 (14.0)	847 (1.2)	804 (3.9)	751 (0.77)
250			1205 (0.72)	1196 (0.44)	1175 (9.9)	1122 (4.0)	1057 (16.2)	1011 (2.93)	988 (5.2)	924 (15.0)	847 (1.0)	806 (3.9)	752 (0.68)
300			1206 (1.5)			1139 (24.7)		1017 (26.3)	980 (0.9)	902 (9.9)	855 (0.83)	810 (0.2)	750 (0.56)
350					1150 (24.2)			1014 (45.6)		889 (5.9)		805 (2.8)	750 (0.4)
400					1154 (14.8)			1015 (72.2)		890 (3.5)		805 (1.5)	750 (0.33)
450					1137 (38.3)			1009 (46.6)		895 (10.6)		810 (2.6)	750 (0.65)

Values in parentheses are percentage relative area.

supports the concept that dehydration is complete by 420 °C.

These results of the variation in intensity of the hydroxyl stretching bands are confirmed by the measurement of the water HOH bending modes centred at around 1630 cm^{-1}. Interestingly two bands may be curve resolved at 1646 and 1617 cm^{-1} in the 100 and 150 °C spectra. Above 150 °C, the latter band is not observed. The 1646 cm^{-1} band is attributed to water co-ordinated to the iron(II). The intensity of this band is lost by 400 °C. Whilst IES is not able to distinguish weight loss steps, the technique does confirm (in line with the MS results) that vivianite is dehydrated by 400 °C. The IES of the phosphate-stretching region are shown in Fig. 3c, and the results of the band component analysis reported in Table 3. The spectra are an overlap of a number of vibrations. The bands in the 1100–1460 cm^{-1} region are attributed to overtone and combination bands. The observation of the types of bands in the IES is quite common. The bands at around 1081, 1050 and 1015 cm^{-1} are assigned to the phosphate PO antisymmetric stretching vibrations. Piriou and Poullen found bands at 1053 and 1018 cm^{-1} and are in agreement with our results [26]. The band at around 923 cm^{-1} is assigned to the symmetric stretching vibration. Two bands are observed at 802 and 750 cm^{-1} may be attributed to water librational modes.

4. Conclusions

High-resolution thermogravimetry coupled to a mass spectrometer was used to measure the dehydration of the mineral vivianite $(Fe^{2+})_3(PO_4)_2{\cdot}8H_2O$. The results of DTGA show that the natural vivianite dehydrates in five steps over the temperature range 105–420 °C. Based upon the percentage weight loss for each step a model with chemical reactions is proposed for the dehydration of vivianite. A comparison is made between synthetic and natural vivianite.

Acknowledgements

The financial and infrastructure support of the Queensland University of Technology Centre for Instrumental and Developmental Chemistry is gratefully acknowledged. The Australian research Council (ARC) is thanked for funding the purchase of the Thermo-Analytical Facility.

References

[1] C.W. Wolfe, Am. Miner. 25 (1940) 738.
[2] V.C. Farmer, Mineralogical Society Monograph 4, The Infrared Spectra of Minerals, 1974.
[3] K. Omori, T. Seki, Ganseki Kobutsu Kosho Gakkaishi 44 (1960) 7.
[4] S.V. Gevork'yan, A.S. Povarennykh, Konst. Svoistva Miner. 7 (1973) 92.
[5] S.V. Gevork'yan, A.S. Povarennykh, Miner. Zh. 2 (1980) 29.
[6] G.R. Hunt, J.W. Salisbury, C.J. Lenhoff, Mod. Geol. 3 (1972) 121.
[7] G.R. Hunt, Geophysics 42 (1977) 501.
[8] R. Sitzia, Rend. Semin. Fac. Sci. Univ. Cagliari 36 (1966) 105.
[9] B. Piriou, J.F. Poullen, J. Raman Spectrosc. 15 (1984) 343.
[10] C.A. Melendres, N. Camillone, T. Tipton, Electrochim. Acta 34 (1989) 281.
[11] R.L. Manly Jr., Am. Mineral. 35 (1950) 108.
[12] J.L. Dormann, M. Gasperin, J.F. Poullen, Bull. Mineral. 105 (1982) 147.
[13] R. Pulou, Compt. Rend. 241 (1955) 221.
[14] K.A. Rodgers, Geol. Mijnbouw 68 (1989) 257.
[15] K.A. Rodgers, G.S. Henderson, Thermochim. Acta 104 (1986) 1.
[16] R.L. Frost, B.M. Collins, K. Finnie, A.J. Vassallo, Clays controlling environment, in: Proceedings of the 10th International Clay Conference, Adelaide, SA, 1995, p. 219.
[17] R.L. Frost, A.M. Vassallo, Clays Clay Miner. 44 (1996) 635.
[18] R.L. Frost, A.M. Vassallo, Mikrochim. Acta Suppl. 14 (1997) 789.
[19] R.L. Frost, J.T. Kloprogge, S.C. Russell, J. Szetu, Appl. Spectrosc. 53 (1999) 829.
[20] R.L. Frost, J.T. Kloprogge, S.C. Russell, J. Szetu, Appl. Spectrosc. 53 (1999) 572.
[21] J.T. Kloprogge, R.L. Frost, Appl. Clay Sci. 15 (1999) 431.
[22] J.T. Kloprogge, R.L. Frost, J. Kristof, Can. J. Anal. Sci. Spectrosc. 44 (1999) 33.
[23] J.T. Kloprogge, R.L. Frost, Neues Jahrb. Mineral. Monatsh 4 (2000) 145.
[24] A.G. Kotlova, N.I. Shchepochkina, Term. Anal. Miner (1978) 45.
[25] M.O. Figueiredo, S. Furtado, J.C. Waerenborgh, Mem. Not., Publ. Mus. Lab, Mineral. Geol. Univ., Coimbra 98 (1984) 83.
[26] B. Piriou, J.F. Poullen, Bull. Mineral. 110 (1987) 697.